de Haas–van Alphen effect and Fermi surface of lutetium

W. R. Johanson* and G. W. Crabtree
Materials Science and Technology Division, Argonne National Laboratory, Argonne, Illinois 60439

F. A. Schmidt
Ames Laboratory, Iowa State University, Ames, Iowa 50010
(Received 21 July 1983)

We report de Haas–van Alphen measurements of the Fermi surface of lutetium at temperatures down to 0.3 K and in fields up to 150 kG in the $(10\bar{1}0)$ and $(11\bar{2}0)$ planes. Lutetium, having a filled $4f$ shell, serves as a nonmagnetic prototype of the structurally similar (hcp), trivalent, heavy rare-earth elements from Gd to Tm. The fact that no complete frequency branches were observed indicates that there are no closed pieces of the Fermi surface. We observed all but one orbit predicted by relativistic augmented-plane-wave calculations of Keeton and Loucks and by recent spin-orbit–linearized-augmented-plane-wave calculations of Tibbetts and Harmon. The data support a geometry similar to that of yttrium, and in good qualitative agreement with energy-band theory.

I. INTRODUCTION

The heavy rare-earth elements, Gd through Lu, are isostructural (hcp) with one another at low temperatures and, with the exception of divalent Yb, in their metallic environments they have three conduction electrons derived from $6s$ and $5d$ atomic states. They differ in number of $4f$ electrons per atom, increasing from 7 for Gd to 14 for Lu. At sufficiently low temperatures, Gd through Tm exhibit various forms of magnetically ordered structures.[1–11] Gd transforms directly from paramagnetic to ferromagnetic, while Tb through Tm each have a temperature range over which an antiferromagnetic modulated-moment phase exists, whose structure may be generally described as a screw-type arrangement of spins with wave vector $\vec{Q}$ along the c axis. For the antiferromagnetic structures, the spacing between parallel portions of the third- and fourth-zone sheets of the Fermi surface has been associated with $\vec{Q}$.[12–17]

The paramagnetic Fermi surfaces of the trivalent heavy rare-earth elements are expected to be quite similar to one another since the same $6s$ and $5d$ conduction electrons are involved in each case and since their lattice constants are similar. Despite this similarity, there can be no measurement of the paramagnetic Fermi surface in any of the heavy rare-earth elements except Lu. The other elements all display low-temperature magnetic order, which modifies the paramagnetic Fermi surface either by introducing exchange splitting of the bands in the case of ferromagnetism, or by introducing extra Brillouin-zone faces due to the larger magnetic unit cell in the case of the modulated-moment systems. The nonmagnetic elements Y and Sc are isoelectronic and isostructural with Lu, suggesting that their Fermi surfaces might serve as models for the heavy rare-earth elements. However, both Y and Sc are considerably lighter atoms where relativistic effects are not expected to be as important as in Lu. In addition, band-structure calculations show small systematic changes in the Fermi surface of the heavy rare-earth elements as one moves across the series, making a rigorous analogy between Y and Sc and the heavy rare-earth elements impossible. As we will show, there are many similarities between the Y and Lu Fermi surfaces, but some important differences exist also. Consequently, Lu is the only element where the paramagnetic heavy rare-earth Fermi surface with the appropriate relativistic modifications can be experimentally explored.

There has been earlier experimental work on the electronic structure of three of the heavy rare-earth elements[18–26] and on Y.[27,28] Experimental and theoretical work on Sc is in progress.[29] Detailed Fermi-surface measurements have been made on ferromagnetic Gd,[18–22] and partial results have appeared for Tb (Ref. 23) and Lu.[24] For Y and Gd, the experimental results generally confirm existing non-self-consistent band-structure calculations,[30–37] while measurements on Tb and the previous work on Lu are not sufficiently complete for serious comparison. A review of experimental work through 1976 has been given by Young,[38] and reviews of theoretical work have been given by Liu,[39] Freeman,[40] and Dimmock.[41] Recently, self-consistent relativistic band calculations of Lu have been carried out by Tibbetts and Harmon.[36,37]

Previous de Haas–van Alphen (dHvA) measurements on Lu (Ref. 24) were made on a single crystal having a resistance ratio of about 60, in pulsed fields up to 200 kG, and yielded only one frequency branch. We present new dHvA measurements on a single crystal having a resistance ratio of 100, in fields up to 150 kG produced by a high homogeneity superconducting magnet and at temperatures down to 0.3 K. We observe a total of seven new frequencies in addition to the single branch reported earlier.[24] We present measurements of the variation of the orbital areas with angle, and of the effective mass and Dingle temperature for selected orbits. A slight misorientation of the crystal for field directions near $\langle 0001 \rangle$ which was noted in a preliminary report of this work[42]

has been corrected. A detailed comparison of our experimental results is made to the band calculations of Tibbitts and Harmon.[36]

II. SAMPLE PREPARATION

Single crystals of lutetium were grown at Ames Laboratory using the arc-zone-melting technique[43,44] and purified by electrotransport in a hydrocarbon-free atmosphere having a pressure not greater than 1.0×10^{-10} Torr. During electrotransport, the temperature of the Lu rod was held at 1100 °C for 430 h. Because of the ease with which Lu twins if stressed, it was necessary to use copper braid for current leads which also functioned as a strain-free flexible support. For dHvA measurements, a piece measuring approximately $0.025\times0.025\times0.050$ in.^{3} was spark-cut from the single-crystal rod and electropolished in a perchloric-acid—methanol solution. The major symmetry directions were determined by Laue diffraction so that the oriented crystal could be rotated *in situ* in either the $(10\bar{1}0)$ or $(11\bar{2}0)$ plane.

III. de HAAS—van ALPHEN MEASUREMENTS

With the exception of a new 150-kG superconducting magnet, the dHvA spectrometer is as described elsewhere.[45–47] The magnet was custom-built to combine high fields with high homogeneity, a requirement for sensitive dHvA measurements. Field profile measurements which utilize NMR on ^{27}Al show the homogeneity near the magnetic center to be 0.09% at 148 kG for 1-cm axial displacement. For routine field measurements, the magnetoresistance of a noninductively wound copper coil calibrated by NMR field measurements was used. dHvA measurements were made using the field modulation technique at 101 Hz with detection on the second harmonic.

Lu has three valence electrons per atom, with two atoms per primitive unit cell of the hexagonal lattice. (This corresponds to six atoms per conventional Bravais unit cell.) There are six conduction electrons per primitive cell, enough to completely fill three of the valence bands. The lowest two valence bands are filled, while bands 3 and 4 are each partially filled. The even number of valence electrons per unit cell implies that Lu is a compensated metal; i.e., there are as many electrons in band 4 as there are holes in band 3. In terms of Fermi-surface geometry, this implies that the occupied volumes of the third and fourth zones add exactly to one zone volume.

Band-structure calculations.[34,36] indicate that the Fermi surfaces in zones 3 and 4 are topologically similar, as indicated in Fig. 1. Each sheet is open along the Γ—A direction, with the occupied region toward the outer rectangular zone faces. If the surface is viewed as containing holes, it looks like a central trunk along Γ—A with flattened arms extending along the six A—L directions on the hexagonal end faces of the zone. The surfaces of these arms approximately parallel to the ΓKM plane make up the "webbing" feature containing the nesting vector $\vec{Q}$ associated with the magnetic order.

In nonrelativistic band calculations the zone-3 and zone-4 surfaces must touch in the basal AHL planes of the Brillouin zone. This degeneracy led to the use of the

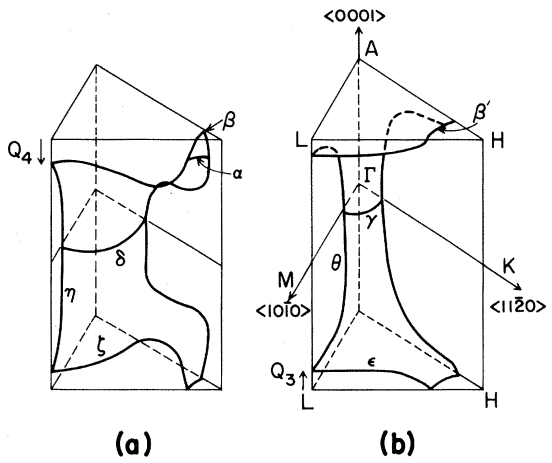

FIG. 1. Fermi surface of Lu in the $\frac{1}{12}$th wedge of the first Brillouin zone; (a) zone 4 and (b) zone 3. The fractions of the nesting vector $\vec{Q}=\vec{Q}_3+\vec{Q}_4$ lying in each zone are labeled.

"double-zone representation" for describing the Fermi surface. This scheme is useful for showing various composite orbits traversing the zone-3 and zone-4 sheets which can occur due to magnetic breakdown across the spin-orbit energy gaps in the AHL plane. However, it was found experimentally in both Y (Ref. 28) and Lu (this work) that the spin-orbit energy gaps in the AHL plane are sufficiently large to prevent magnetic breakdown at all experimentally accessible fields, so that the double-zone representation is not useful for these cases and we will not employ it in this paper. Instead, we view both sheets of the Fermi surface in a single reduced zone, with the zone-3 sheet lying inside the zone-4 sheet. Since neither sheet is closed, the terms electron and hole cannot be unambiguously applied to either of them. This terminology has occasionally appeared in earlier work, with the zone-3 surface often depicted as containing holes and the zone-4 surface as containing electrons. In this paper we will refer to the surfaces simply as zone 3 and zone 4. Particular cyclotron orbits on each surface will be designated as electron or hole according to whether they enclose occupied or unoccupied regions of the Brillouin zone.

The similar topology of the zone-3 and zone-4 sheets implies that the same generic types of orbits appear on both sheets. In addition, many of these same orbits appear in Y and Sc. The earlier thorough descriptions of the Fermi surface and cyclotron orbits in Y (Ref. 28 and 33) are useful for visualizing and analyzing the Fermi surface of Lu. To make comparison easier, Table I shows the orbit designations and experimental areas and masses for Y and for the present work on Lu. Each orbit, specified by a field direction and orbit center, may appear as many as four times in the table: once in each of zone 3 and zone 4 for Y and for Lu. The angular dependence of the observed cross-sectional areas for Lu in the $(10\bar{1}0)$ and $(11\bar{2}0)$ planes is shown in Fig. 2. The notation for the symmetry points and directions in the hexagonal Brillouin zone in shown in Fig. 1(b).

Oscillations of the γ and δ orbits were observed only

TABLE I. Comparison of experimental cross-sectional areas and effective masses for Y [Mattocks and Young (Ref. 28)] and Lu (this work). Dingle temperatures are shown for the three orbits in zone 4 where measurements were taken.

			Zone 3					Zone 4					
			Lu		Y			Lu			Y		
$\hat{H}$	Orbit center	Orbit type	Area (a.u.)	Mass m^*/m_0	Area (a.u.)		Mass m^*/m_0	Area (a.u.)		Mass m^*/m_0	X (K)	Area (a.u.)		Mass m^*/m_0
⟨0001⟩	Γ	hole	0.095	γ	0.151	α	2.4	0.45	δ			b	γ	
	Γ–A	hole		a	0.130	β	2.7		a				a	
	H	electron	b	β'	0.0125	δ_3	0.53	0.017[c]	β	0.9[c]		0.0106	δ_2	0.39
	H–K	electron		a		a		0.010	α	0.42[c]	1.8[c]	0.00861	δ_1	0.39
⟨10$\bar{1}$0⟩	L	hole	0.030	ϵ	1.7	0.0575	ϵ_2	2.4	0.085	ζ	2.6	1.0	0.0762	ϵ_3	2.4
	A–L	hole		a		0.0468	ϵ_m	2.4		a				a	
⟨11$\bar{2}$0⟩	M	electron	0.30	θ		0.278	ζ		0.114	η	3.0	1.2	0.0968	η	1.6
	A–K	hole				0.109	κ^1	3.9							
	M–K	electron				b	θ							a	

[a]Not predicted.
[b]Predicted but not observed.
[c]15° from ⟨0001⟩ toward ⟨10$\bar{1}$0⟩.

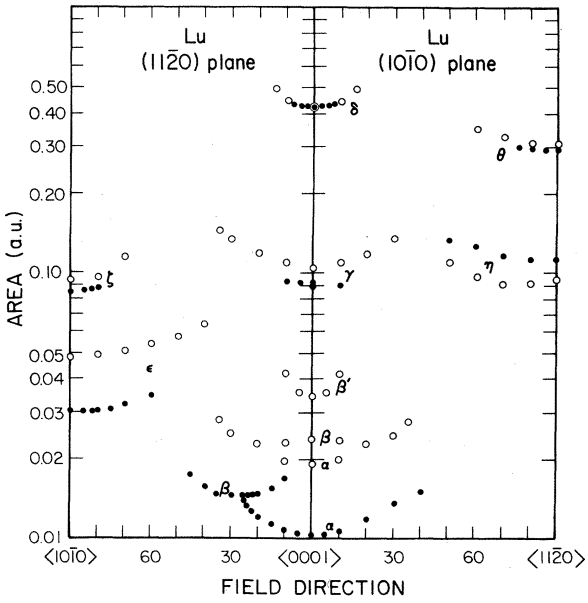

FIG. 2. Comparison of experimental and theoretical cross-sectional areas of the Fermi surface of Lu as a function of angle for the (10$\bar{1}$0) and (11$\bar{2}$0) planes. Solid circles, experimental; open circles, band structure of Tibbetts and Harmon (Ref. 36).

above 130 kG at temperatures below 0.5 K, and even under these favorable conditions had very small amplitudes. γ was especially weak. The small amplitudes for γ and δ are consistent with the heavy masses predicted by Tibbetts and Harmon,[36] as discussed in Sec. IV, and with the large mass[28] measured on the orbit corresponding to γ in Y.

The areas of all branches turn upward with field direction before their amplitudes diminish to zero, consistent with an open surface geometry. There is no evidence supporting a closed Fermi surface, since we found no branches extending continuously from ⟨0001⟩ to the basal plane.

Effective masses were obtained from the temperature dependence of the amplitudes at a fixed value of field and are given in Table I. Hoekstra and Phillips[24] measured a mass of 0.39 on the α orbit, in reasonably close agreement with our measurement of 0.42. The amplitude of the oscillations from γ, δ, and θ were too low for their masses to be measured. Dingle temperatures, a measure of the electron scattering lifetime, were obtained from the field dependence of the amplitudes and are also given in Table I for certain orbits on the zone-4 sheet.

Table I shows several differences between the Fermi surfaces of Y and Lu. In zone 4 the γ orbit in Y was not observed, although the topology of the Fermi surface demands that it be present. We observe the corresponding orbit in Lu, δ, but only weakly as discussed above. In zone 3, the noncentral β orbit in Y is not predicted to exist in Lu, nor is it observed. This indicates that the cross-sectional area of the trunk is more nearly constant along the Γ–A axis near the ΓKM plane in Lu than in Y. Our experiments do not show any analog in Lu to the noncen-

TABLE II. Comparison of experimental and theoretical cross-sectional areas and masses in Lu.

Field direction	Orbit	Experimental			Theoretical		
		Hoekstra and Phillips (Ref. 24) Area (a.u.)	This work Area (a.u.)	This work mass m^*/m_0	Keeton and Loucks (Ref. 34) Area (a.u.)	Tibbetts and Harmon (Ref. 36) Area (a.u.)	Tibbetts and Harmon (Ref. 36) mass m^*/m_0
⟨0001⟩	α	0.010	0.010	0.42[a]		0.019	0.38
⟨0001⟩	β		0.017[a]	0.9[a]	0.021	0.023	0.65
⟨0001⟩	β'				0.03	0.036	0.74
⟨0001⟩	γ		0.095		0.10	0.10	1.3
⟨0001⟩	δ		0.45		0.46	0.43	3.9
⟨11$\bar{2}$0⟩	η		0.114	3.0	0.08	0.097	1.7
⟨11$\bar{2}$0⟩	θ		0.30		0.34	0.31	2.2
⟨10$\bar{1}$0⟩	ϵ		0.030	1.7	0.045	0.048	0.86
⟨10$\bar{1}$0⟩	ζ		0.085	2.6	0.11	0.094	1.3

[a] 15° from ⟨0001⟩ toward ⟨10$\bar{1}$0⟩.

tral ϵ_m orbit in Y, implying that the cross-sectional areas of the flattened arms in zone 3 and zone 4 do not increase as the L point is approached from A. We did not observe in Lu any analog to the κ^1 orbit of Y, although the topology of the Fermi surface strongly suggests that it should exist. However, this orbit probably has a large effective mass (the κ^1 orbit in Y has a mass of 3.9) and an unfavorable curvature factor, making its observation difficult. The corresponding orbit in zone 4 was not seen in Y or in Lu. Likewise, the noncentral θ orbit predicted by band theory in zone 3 of Y was not seen in Y or in Lu. Finally, the β' orbit in Lu, corresponding to the δ_3 orbit in zone 3 of Y, was not observed. This will be discussed in more detail in Sec. IV.

The effective masses in Lu differ from those of Y. Table I shows that the masses in zone 4 are larger in Lu than in Y, especially on the β and η orbits. For the single orbit in zone 3 where comparison is possible, the mass is smaller in Lu than in Y. In general, the masses in Y and Lu are expected to be comparable, though slightly larger in Y, as indicated by electronic specific-heat measurements and band-structure calculations of the electronic density of states. Specific-heat measurements show values of γ near 8.2 mJ/mol K^2 for Lu (Refs. 48 and 49) and 10.2 mJ/mol K^2 for Y,[50–53] while band calculations predict values of the density of states of 23.5 states/atom Ry for Lu (Refs. 34 and 37) and 26.8 states/atom Ry for Y.[33] These data imply an average enhancement of the masses of 2.0 for Lu and 2.2 for Y. It is surprising that despite these large enhancements, neither Lu nor Y is a good superconductor [$T_c \leq 0.1$ K for Lu (Ref. 54) and $T_c < 0.005$ K for Y (Ref. 55)]. Apparently the large mass enhancements in these metals include significant repulsive many-electron interactions in addition to the attractive electron-phonon interaction.

IV. COMPARISON WITH BAND STRUCTURE

Non-self-consistent relativistic augmented-plane-wave (RAPW) calculations were performed by Keeton and Loucks[34] for paramagnetic Gd, Dy, Er, and Lu. Recently Tibbetts and Harmon[36,37] have performed self-consistent spin-orbit—linearized-APW (SO-LAPW) calculations on Lu, treating the non-spin-orbit relativistic effects in the initial step and including the spin-orbit coupling as a second variation.[56] The results of Tibbetts and Harmon for the angular variation of cross-sectional areas are shown together with our dHvA data in Fig. 2. The theoretical cross-sectional areas obtained by Keeton and Loucks (estimated) and by Tibbetts and Harmon are tabulated in Table II along with the current dHvA results and the earlier results of Hoekstra and Phillips.[24] The areas attributed to Keeton and Loucks were estimated graphically from their partial Fermi-surface cross sections. Using lattice constants $a=3.50$ Å and $c=5.50$ Å, which yield Brillouin-zone areas $A(ALH)=0.087$ a.u., $A(\Gamma ALM)=0.164$ a.u., and $A(LHKM)=0.095$ a.u., we arrive at the estimates given in column six of Table II. Inspection of Table II shows that both theoretical results give qualitatively the same Fermi-surface geometry in agreement with our dHvA data. The calculations of Tib-

betts and Harmon give somewhat better quantitative results for α, η, θ, ζ, and a slightly worse result for ϵ.

In both band calculations the cylindrical surfaces surrounding $\langle 0001 \rangle$ curve outward parallel to the basal plane, and give rise to cross-sectional areas that increase more rapidly with angle than would those of a smooth cylinder, consistent with the measured angular dependence of the γ, δ, ϵ, and α orbits. The experimental uncertainty in θ is too large to allow any statement regarding the rate of change of its area with angle to be made.

The structure of the Fermi surface near the $H-K$ line in zone 4 differs in the calculations of Tibbetts and Harmon[36,37] and of Keeton and Loucks.[34] The latter authors find a single, minimum area orbit centered at H for the field direction along $\langle 0001 \rangle$. In contrast, Tibbetts and Harmon find two orbits in zone 4, labeled α and β in Fig. 1. The β orbit, centered at H, is a maximum orbit, while a smaller minimum orbit α is centered on the $H-K$ line away from H. This structure is qualitatively similar to that in zone 4 of Y. Both sets of authors predict a single orbit β' in zone 3 of Lu, centered at H and analogous to the δ_3 orbit of Y.

The experimental data are most consistent with the calculation of Tibbetts and Harmon. The observed β orbit cannot be associated with the zone-3 orbit β' because the angular dependence of its area and the angular range over which it is observed are not appropriate. Thus, in the Keeton and Loucks calculation, there is no interpretation for the observed β orbit. The observed α orbit area rises faster than that of a cylinder as the field is tipped off $\langle 0001 \rangle$, implying that it is a minimum orbit. The α orbit joins smoothly with β in the $(11\bar{2}0)$ plane, as predicted qualitatively by Tibbetts and Harmon. Furthermore, we find the effective masses of α and β to be 0.42 and 0.9, respectively, similar to the predicted values[36] of 0.38 and 0.65 if a reasonable mass enhancement is assumed. These mass values are significant because they differ from those of Y, where the δ_1 and δ_2 orbits were found[28] experimentally to have the same mass, 0.39.

Within the Tibbetts and Harmon interpretation we cannot explain why the H centered β orbit is not seen all the way to $\langle 0001 \rangle$ in the $(11\bar{2}0)$ plane, nor why β is not seen in the $(10\bar{1}0)$ plane. We speculate that the zone-4 surface in the neighborhood of H is highly distorted, producing an unfavorable curvature factor for the β orbit. As support for this speculation, we note that the α orbit rises appreciably faster in the $(11\bar{2}0)$ plane than in the $(10\bar{1}0)$ plane, and that the extrapolated areas of the α and β orbits differ by more than 70% at $\langle 0001 \rangle$. Neither of these features is seen in the band theory for Lu nor in the experiments on Y. In both cases the area behavior of the two orbits near $\langle 0001 \rangle$ is very nearly the same in both the $(10\bar{1}0)$ and $(11\bar{2}0)$ planes, and the area difference between the central and noncentral orbits at $\langle 0001 \rangle$ is only 20%. As noted by Tibbetts and Harmon,[36] and by Loucks,[33] the bands near the H point are very flat and the Fermi surface in this region is sensitive to small changes in the potential, for example, due to non-muffin-tin effects.

Similar geometrical arguments apply to the β' orbit, which was not observed despite a careful search for it. Band-structure calculations[34,36] of Lu explicitly show that the zone-3 Fermi surface is sharply curved near H as the AHL face of the Brillouin zone is approached from K, as illustrated in Fig. 1(b). This implies that β' will have an unfavorable curvature factor and exist over a rather narrow angular range for fields near $\langle 0001 \rangle$. In addition, the Dingle temperatures for the small orbits centered on the $H-K$ line may be rather high, as indicated in Table I for the α orbit. Unfavorable curvature factors for β and β', high Dingle temperatures, and relatively high masses ($m^*=0.65$ and 0.74 for β and β' in the band calculation of Lu versus 0.39 and 0.53 measured for the corresponding orbits in Y) may make the signals too weak to observe.

Comparison of the theoretical and experimental effective masses in Table II shows that the larger area orbits have a mass enhancement close to the average value of 2.0 derived at the end of Sec. III. This correspondence suggests that the reason for the weak signals associated with the γ, δ, and θ orbits is their relatively large enhanced effective masses, expected to be 2.6, 7.8, and 4.4, respectively, based on the values of the band masses. The lower apparent enhancement of masses of the smaller area orbits may be an artifact of the band calculation due to the sensitivity of the calculated Fermi surface near the H point to small changes in the potential, as noted above. The calculated areas of the α and β orbits are too large. If the areas are adjusted downward, the calculated effective masses will also decrease. If the slopes of the bands are held constant while the areas are reduced, the masses scale with the square root of the area. For the α orbit, an adjustment in area of nearly a factor of 2 is required, which would lower the calculated mass to a value much more consistent with the averge enhancement of 2.0. A similar adjustment of the β orbit area and mass would bring its enhancement closer to the average, but quantitative estimates are difficult to make because the observed and calculated orbits are for slightly different field directions.

A key feature of our results is the existence of the ζ and ϵ orbits, which, in conjunction with band-structure results, we interpret as being L centered on the nested zone-3 and zone-4 sheets. It has been proposed that the separation between these two sheets across the AHL plane along $M-L$ determines the spatial period of the particular modulated-moment structure,[12–17] and when the ordering occurs, the parts of the surface perpendicular to $\langle 0001 \rangle$ are destroyed by the introduction of superzone boundaries, while those parallel to $\langle 0001 \rangle$ remain, but in a somewhat modified fashion.[12,13,16,57]

The Q vector describing the modulated magnetic order is related to the band structure through the $\vec{q}$-dependent susceptibility $\chi(\vec{q})$. Calculations of $\chi(\vec{q})$ which utilize the bands of Tibbetts and Harmon[36] and of Keeton and Loucks[14,17,34] assuming constant matrix elements give a peak in $\chi(\vec{q})$ at $Q=0.54\pi/c$, very close to the length of the nesting vector separating the zone-3 and zone-4 surfaces along the $M-L$ line. Since the Fermi-surface geometry is the most important factor governing the position of the peaks in $\chi(\vec{q})$, we may adjust the theoretical value of Q using the experimental areas of the ϵ and ζ orbits. Both measured areas are smaller than predicted by theory, implying that the length of the nesting vector and position of the peak in $\chi(\vec{q})$ have been overestimated. If

the shapes of the theoretical ϵ and ζ orbits are kept fixed while the sizes are reduced until the areas agree with experiment, the contribution of the zone-4 sheet to the nesting vector along the $M-L$ line is reduced by 5%, the contribution of the zone-3 sheet to the nesting vector is reduced by 21%, and the total length of the nesting vector is reduced by 11% to $0.48\pi/c$. The experimental ordering vector obtained by extrapolation from measurements on Lu$\mathscr{R}$ alloys[1] (where $\mathscr{R}$ represents a rare-earth element) is $0.53\pi/c$. Although these geometrical corrections to Q degrade the agreement with experiment, the agreement is still very satisfactory in view of the approximation of constant matrix elements in the calculation of $\chi(\vec{q})$.

V. CONCLUSIONS

We present data over an extensive portion of the Lu Fermi surface, the best prototype surface for the elements Gd through Tm in their paramagnetic phases. The data support a Fermi-surface geometry qualitatively similar to that of isoelectronic Y,[27,28] consisting of two nested sheets with a webbing feature centered at L. The surface is in good qualitative agreement with RAPW calculations of Keeton and Loucks,[34] but recent self-consistent SO-LAPW calculations by Tibbetts and Harmon[36] provide somewhat better quantitative agreement. The data support the existence of L-centered orbits arising from the webbing at L which has been associated with magnetic ordering of elements Tb through Tm.[34]

ACKNOWLEDGMENTS

We thank our colleagues and friends Dr. Bruce Harmon, Dr. Dale Koelling, and Dr. James Schirber for several helpful and stimulating discussions and comments. This work was performed at Argonne National Laboratory, which is operated by The University of Chicago for the U.S. Department of Energy under Contract No. W-31-109-ENG-38, and at Ames Laboratory, which is operated by Iowa State University for the U.S. Department of Energy under Contract No. W-7405-ENG-82. This work was supported by the U.S. Department of Energy.

*Present address: Department of Physics, Pomona College, Claremont, CA 91711.

[1]W. C. Koehler, J. Appl. Phys. 36, 1078 (1965).

[2]W. C. Koehler, E. O. Wollan, M. K. Wilkinson, and J. W. Cable, *Proceedings of the First Rare-Earth Conference, 1960* (MacMillan, New York, 1961).

[3]A. R. Mackintosh, *Proceedings of the Second Rare-Earth Conference, 1961* (Gordon and Breach, New York, 1962).

[4]W. C. Koehler, J. Appl. Phys. (Suppl.) 32, 20S (1961).

[5]S. H. Liu, in *Handbook of Physics and Chemistry of the Rare-Earths,* edited by K. A. Gschneidner, Jr. and L. Eyring (North-Holland, Amsterdam, 1978), Vol. 1, Chap. 3.

[6]J. Crangle, *The Magnetic Properties of Solids,* Vol. 6 of *The Structure and Properties of Solids* (Arnold, London, 1977), Chap. 3.

[7]B. Coqblin, *The Electronic Structure of Rare-Earth Metals and Alloys: The Magnetic Heavy Rare-Earths* (Academic, London, 1977), Chap. 2.

[8]H. Miwa, Prog. Theor. Phys. 27, 208 (1962).

[9]R. J. Elliott and F. A. Edgewood, Proc. Phys. Soc. 81, 846 (1963).

[10]R. Nathans and S. J. Pickart, in *Magnetism,* edited by G. T. Rado and H. Suhl (Academic, New York, 1963), Vol. 3, pp. 239–269.

[11]K. Yosida and A. Watabe, Prog. Theor. Phys. 28, 361 (1962).

[12]A. R. Mackintosh, Phys. Rev. Lett. 9, 90 (1962).

[13]H. Miwa, Prog. Theor. Phys. 29, 477 (1963).

[14]W. E. Evenson and S. H. Liu, Phys. Rev. 178, 783 (1969).

[15]R. W. Williams, T. L. Loucks, and A. R. Mackintosh, Phys. Rev. Lett. 16, 168 (1966).

[16]A. J. Freeman, J. O. Dimmock, and R. E. Watson, Phys. Rev. Lett. 16, 94 (1966).

[17]S. H. Liu, R. P. Gupta, and S. K. Sinha, Phys. Rev. B 4, 1100 (1971).

[18]R. C. Young, R. G. Jordan, and D. W. Jones, J. Phys. F 6, L37 (1976).

[19]R. C. Young, R. G. Jordan, and D. W. Jones, Phys. Rev. Lett. 31, 1473 (1973).

[20]R. C. Young and J. K. Hulbert, Phys. Lett. 47A, 367 (1974).

[21]J. E. Schirber, F. A. Schmidt, B. N. Harmon, and D. D. Koelling, Phys. Rev. Lett. 36, 448 (1976).

[22]P. G. Mattocks and R. C. Young, J. Phys. F 7, 1219 (1977).

[23]P. G. Mattocks and R. C. Young, J. Phys. F 7, L19 (1977).

[24]J. A. Hoekstra and R. A. Phillips, Phys. Rev. A 4, 4184 (1971).

[25]R. W. Williams and A. R. Mackintosh, Phys. Rev. 168, 679 (1968).

[26]C. Stassis, G. R. Kline, C.-K. Loong, and B. N. Harmon, Solid State Commun. 23, 159 (1977).

[27]R. C. Young, R. G. Jordan, D. W. Jones, and V. J. Hems, J. Phys. F 4, L84 (1974).

[28]P. G. Mattocks and R. C. Young, J. Phys. F 8, 1417 (1978).

[29]J. E. Schirber and A. C. Switendick, Bull. Am. Phys. Soc. 28, 386 (1983); B. N. Harmon, D. K. Misemer, C. M. Theisen, and C. K. Loong, *ibid.* 28, 386 (1983).

[30]J. O. Dimmock and A. J. Freeman, Phys. Rev. Lett. 13, 750 (1964).

[31]B. N. Harmon and A. J. Freeman, Phys. Rev. B 10, 1979 (1974).

[32]B. N. Harmon and A. J. Freeman, Phys. Rev. B 10, 4849 (1974).

[33]T. L. Loucks, Phys. Rev. 144, 504 (1966).

[34]S. C. Keeton and T. L. Loucks, Phys. Rev. 168, 672 (1968).

[35]C. Jackson, Phys. Rev. 178, 949 (1969).

[36]T. A. Tibbitts and B. N. Harmon, Solid State Commun. 44, 1409 (1982).

[37]T. A. Tibbetts, M. S. thesis, Iowa State University, 1982.

[38]R. C. Young, Rep. Prog. Phys. 40, 1123 (1977).

[39]S. H. Liu, in *Handbook on Physics and Chemistry of the Rare-Earths,* Ref. 5, Vol. 1, Chap. 3.

[40]A. J. Freeman, in *Magnetic Properties of Rare Earth Metals,* edited by R. J. Elliot (Plenum, London, 1972), p. 245.

[41]J. O. Dimmock, in *Solid State Physics,* edited by H. Ehrenreich, F. Seitz, and D. Turnbull (Academic, New York, 1971), Vol. 26, p. 104.

[42]W. R. Johanson, G. W. Crabtree, and F. A. Schmidt, J. Appl.

Phys. 53, 2041 (1982).
[43]O. N. Carlson, F. A. Schmidt, and W. M. Paulson, Trans. Am. Soc. Mat. 57, 356 (1964).
[44]D. T. Peterson and F. A. Schmidt, J. Less-Common Met. 18, 111 (1969).
[45]L. R. Windmiller and J. B. Ketterson, Rev. Sci. Instrum. 39, 1672 (1978).
[46]R. W. Stark and L. R. Windmiller, Cryogenics 8, 272 (1968).
[47]D. P. Karim, J. B. Ketterson, and G. W. Crabtree, J. Low Temp. Phys. 30, 389 (1978).
[48]D. K. Thome, K. A. Gschneidner, G. S. Mowry, and J. F. Smith, Solid State Commun. 25, 297 (1978).
[49]W. A. Taylor, M. B. Levy, and F. H. Spedding, J. Phys. F 8, 2293 (1978).
[50]F. Heiniger, E. Bucher, and J. Muller, Phys. Kondens. Mater. 5, 243 (1966).
[51]T. Satoh and T. Ohtsuka, Phys. Lett. 20, 565 (1966).
[52]F. J. Morin and J. P. Maita, Phys. Rev. 129, 1115 (1963).
[53]H. Montgomery and G. P. Pell, Proc. Phys. Soc. London, Sect. A 78, 622 (1961).
[54]E. I. Nikulin, Fiz. Tverd. Tela (Leningrad) 17, 2795 (1975) [Sov. Phys.—Solid State 17, 1864 (1975)].
[55]B. W. Roberts, J. Phys. Chem. Ref. Data 5, 729 (1976).
[56]A. H. MacDonald, W. E. Pickett, and D. D. Koelling, J. Phys. C 13, 2675 (1980).
[57]M. J. Zuckermann and L. M. Falicov, in *Proceedings of the Tenth International Conference on Low Temperature Physics,* edited by A. S. Borovik-Romanov and V. A. Tulin (Nauka, Moscow, 1967).